

Aberrant light directly impairs mood and learning through melanopsin-expressing neurons

Tara A. LeGates^{1*}, Cara M. Altimus^{1*}, Hui Wang², Hey-Kyoung Lee², Sunggu Yang², Haiqing Zhao¹, Alfredo Kirkwood², E. Todd Weber³ & Samer Hattar^{1,2}

The daily solar cycle allows organisms to synchronize their circadian rhythms and sleep-wake cycles to the correct temporal niche¹. Changes in day-length, shift-work, and transmeridian travel lead to mood alterations and cognitive function deficits². Sleep deprivation and circadian disruption underlie mood and cognitive disorders associated with irregular light schedules². Whether irregular light schedules directly affect mood and cognitive functions in the context of normal sleep and circadian rhythms remains unclear. Here we show, using an aberrant light cycle that neither changes the amount and architecture of sleep nor causes changes in the circadian timing system, that light directly regulates mood-related behaviours and cognitive functions in mice. Animals exposed to the aberrant light cycle maintain daily corticosterone rhythms, but the overall levels of corticosterone are increased. Despite normal circadian and sleep structures, these animals show increased depression-like behaviours and impaired hippocampal long-term potentiation and learning. Administration of the antidepressant drugs fluoxetine or desipramine restores learning in mice exposed to the aberrant light cycle, suggesting that the mood deficit precedes the learning impairments. To determine the retinal circuits underlying this impairment of mood and learning, we examined the behavioural consequences of this light cycle in animals that lack intrinsically photosensitive retinal ganglion cells. In these animals, the aberrant light cycle does not impair mood and learning, despite the presence of the conventional retinal ganglion cells and the ability of these animals to detect light for image formation. These findings demonstrate the ability of light to influence cognitive and mood functions directly through intrinsically photosensitive retinal ganglion cells.

In mammals, all light information for image formation and regulation of behaviour is detected by the retina and signalled to the relevant brain targets through retinal ganglion cells (RGCs). Most RGCs signal light to thalamic relay nuclei and then to the visual cortex for image functions. A population of intrinsically photosensitive RGCs (ipRGCs^{3,4}), which predominantly signal light information for non-image-forming visual functions, expresses the photopigment melanopsin and can be distinguished from most RGCs that support image tracking and detection⁵. ipRGCs project to several hypothalamic and preoptic areas such as the suprachiasmatic nucleus (SCN), subparaventricular nucleus and ventrolateral preoptic area to regulate circadian rhythms and sleep. However, they also project to limbic regions such as the lateral habenula and the medial amygdala^{4,6}, highlighting a possible role in the regulation of cognitive functions.

To determine how aberrant light influences behaviour, we subjected mice to an ultradian cycle consisting of 3.5-h light and 3.5-h dark (T7). Our previous studies showed that this T7 aberrant light cycle does not affect the architecture (Supplementary Fig. 1) or the total sleep levels when compared to a 12 h:12 h light-dark (T24) control cycle⁷. We also determined whether the circadian timing system was disrupted in the

T7 animals by measuring core body temperature and general activity rhythms. The T7 cycle does not cause circadian arrhythmicity in either output rhythm (Fig. 1a, b and Supplementary Fig. 2), although the circadian period is lengthened.

To determine whether the T7 cycle influences the molecular basis of the circadian clock, we measured circadian changes of a molecular clock component (PER2) in central (SCN) and peripheral (liver) tissues. Mice housed in the T7 cycle show similar rhythms and localization of PER2 expression in the SCN as in littermates housed in the T24 cycle (Fig. 1c and Supplementary Fig. 3), indicating no disruption of internal rhythmicity of the SCN pacemaker. Furthermore, *Per2* levels in the liver from mice housed in the T24 or T7 light cycle were intact and showed similar phases (Fig. 1d). Together, these data show that the T7 light cycle does not disrupt sleep or cause circadian arrhythmicity. Although the circadian timing system and sleep remain intact under the T7 light cycle, mice are exposed to light pulses at all circadian phases during the experimental time course owing to the mismatch between the imposed light cycle and the period length. Thus, the T7 cycle will allow us to determine the direct influence of aberrant light exposure on mood and cognitive functions.

The T7 model causes light to appear during the night (active) phase of the animals' cycle. To determine which brain regions respond to light presented at night, we measured expression of the transcription factor *c-Fos* in response to an acute light pulse. After examination of ipRGC targets that are part of or known to influence the limbic system, we found light-induced *c-Fos* expression in the amygdala, lateral habenula and subparaventricular nucleus (Supplementary Fig. 4). This suggests that light input particularly when presented at an aberrant time of day may influence regions of the brain involved in mood and cognitive functions.

Shorter day-length during the winter months leads to a seasonal form of depression known as seasonal affective disorder (SAD), and appropriately timed light therapy can alleviate the symptoms of SAD⁸. We thus investigated whether the T7 cycle, which exposes animals to light at inappropriate times, causes depression-like behaviours in mice by evaluating sucrose anhedonia and behavioural despair in the forced swim test (FST). Mice housed in the T7 cycle showed decreased sucrose preference, indicating an increase in depression-like behaviour (Fig. 1e and Supplementary Fig. 5). This was further supported by the FST; mice housed in the T7 cycle spent significantly more time immobile than mice housed in the T24 cycle (Fig. 1f).

An established association with depression is increased serum corticosterone levels⁹. We measured serum corticosterone in animals housed in T24 or T7 cycles at four time points across the day. Although we found an intact circadian rhythm in corticosterone with a similar phase to mice housed in the T24 cycle, the overall levels of corticosterone were increased in mice housed in the T7 light cycle (Fig. 1g).

Increases in corticosterone levels as well as anhedonia are correlated with increased stress and anxiety¹⁰. To assay anxiety-like behaviour, we

¹Department of Biology, Johns Hopkins University, Baltimore, Maryland 21218, USA. ²Department of Neuroscience, Johns Hopkins University, Baltimore, Maryland 21218, USA. ³Department of Biology, Rider University, Lawrenceville, New Jersey 08648, USA.

*These authors contributed equally to the work.

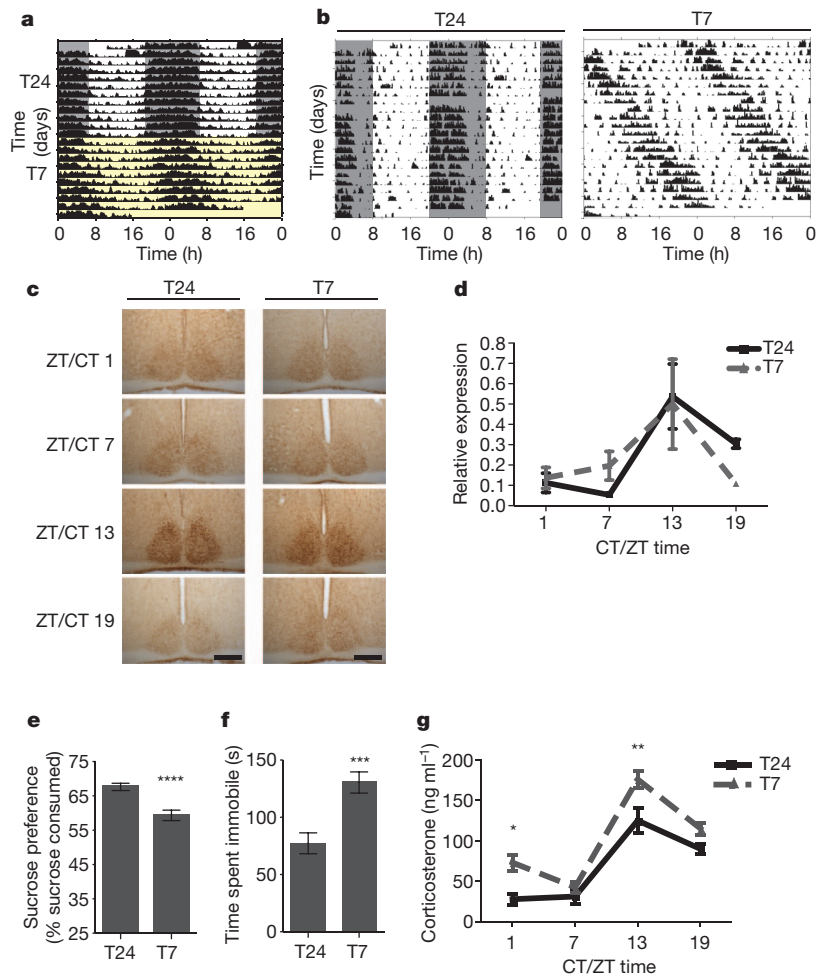


Figure 1 | Aberrant light increases depression-like behaviour and corticosterone levels. **a**, Body temperature rhythms under the T24 (grey/white) and T7 (yellow) cycles. **b**, General activity rhythms under the T24 (left) and T7 (right) cycles. **c**, PER2 expression in the SCN was rhythmic under the T24 and T7 cycles. Scale bars, 200 μm . **d**, Liver *Per2* expression was rhythmic ($P_{\text{time}} = 0.0072$) ($n = 3\text{--}4$ per time point, $P_{\text{light cycle}} = 0.8482$). CT, circadian

time; ZT, zeitgeber time. **e**, T7 mice showed sucrose anhedonia ($n = 16$ (T24) and $n = 15$ (T7), $P < 0.0001$). **f**, T7 mice showed increased immobility in the FST ($n = 22$ per group, $P = 0.0002$). **g**, Corticosterone levels were rhythmic but increased in T7 mice ($n = 5\text{--}6$ per time point, $P_{\text{time}} < 0.0001$, $P_{\text{light cycle}} < 0.0001$, Bonferroni post-test: $P < 0.05$ ZT/CT 1 and $P < 0.01$ ZT/CT 13). * $P < 0.05$; ** $P < 0.01$; *** $P < 0.001$; **** $P < 0.0001$. Error bars indicate s.e.m.

used three tests: open field test, light-dark box and elevated plus maze. We found no significant difference between animals maintained in the T24 cycle and those in the T7 cycle (Supplementary Fig. 6). These results show that the T7 cycle does not globally influence behaviour but specifically elicits depression- and not anxiety-like behaviours.

Increased serum corticosterone levels and depression have been closely associated with hippocampal learning deficits¹¹. We conducted a hippocampal-dependent task, the Morris water maze (MWM) (Fig. 2a–d). In the MWM, the T7 mice required significantly more trials to achieve the same latency in locating a hidden platform compared with the T24 mice (Fig. 2b), despite similar swim speeds. All our measurements were done during the day in the T24 mice (Supplementary Fig. 7). Previous studies using the MWM have shown that mice use a hippocampal-dependent spatial strategy and a hippocampal-independent non-spatial strategy to locate the platform¹². We sought to determine whether the deficit in learning acquisition in the T7 mice was due to the lack of hippocampal-dependent spatial learning. We therefore conducted a probe trial, in which the platform in the water maze was removed from the target quadrant¹³ (Fig. 2c). We found that mice housed in the T24 cycle showed a significant preference for the target quadrant, whereas mice housed in the T7 cycle showed no preference for the target quadrant (Fig. 2c). Using a reversal assay, mice housed in the T24 cycle required significantly more trials to locate

the platform in the new quadrant, whereas the T7 mice showed no change in the latency to locate the platform (Fig. 2d). This further supports the dependence of T7 mice on a non-spatial escape strategy, highlighting a hippocampal-dependent learning deficit.

Spatial learning deficits are usually associated with long-term potentiation (LTP)¹⁴ decrement in the hippocampus. We found that mice housed in both the T24 and T7 cycles have similar basal synaptic transmission at the Schaffer collaterals in the hippocampus (Fig. 2e, f). However, mice housed in a T7 cycle showed impaired LTP in response to both one and four pulses of theta burst stimulation (TBS; Fig. 2g, h). We found no difference in low-frequency stimulation-induced long-term depression (LTD) between mice housed in the T24 and T7 cycles (Fig. 2i). Impaired LTP with no change in LTD has been previously associated with sleep deprivation¹⁵. The selective LTP deficits observed in mice housed in the T7 aberrant light cycle independent of sleep deprivation indicates that learning impairments due to inappropriate light exposure and sleep deprivation may use similar neural pathways (see model in Supplementary Fig. 13).

To determine whether the learning deficits in the T7 cycle extend to tasks involved in hippocampal-dependent recognition memory, we conducted the novel object recognition test¹⁶. Mice housed in the T24 cycle showed a significant preference for the novel object (Fig. 2j). By contrast, mice housed in the T7 cycle showed no preference for a novel object from a familiar object (Fig. 2j).

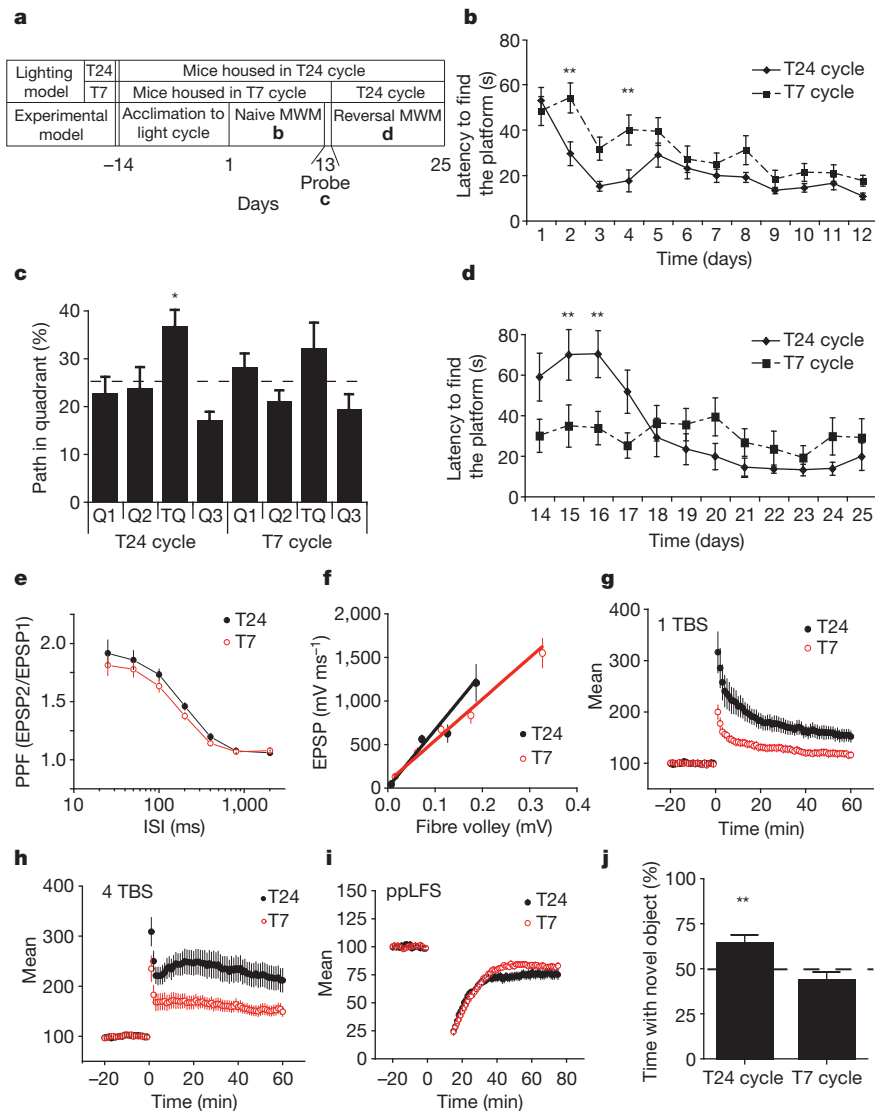


Figure 2 | Aberrant light impairs hippocampal learning, LTP, and recognition memory. **a**, Experimental model for the MWM. **b**, T7 mice showed impaired learning ($n = 21$ per group, $P_{\text{interaction}} = 0.041$, Bonferroni post-test $P < 0.01$ days 2 and 4). **c**, T7 mice show no significant preference for the target quadrant (TQ) (T24: $n = 9$, $P = 0.011$; T7: $n = 9$, $P = 0.25$). Dotted line indicates chance (25%). **d**, Mice housed in the T24 cycle showed an increased latency in a reversal trial, whereas T7-housed mice show a similar latency to the acquisition phase ($n = 9$ per group, $P_{\text{interaction}} < 0.0003$, Bonferroni post-test: $P < 0.01$ days 15 and 16). **e**, **f**, T24 and T7 mice have

To investigate whether antidepressants could rescue the learning deficits observed in T7 mice, we chronically administered fluoxetine to T24 and T7 mice (Fig. 3a). Chronic fluoxetine treatment decreased depression-like behaviour in mice housed in the T7 cycle (Fig. 3b). Furthermore, this treatment was able to rescue the learning deficit observed in the novel object recognition test (Fig. 3c). In support of this behavioural rescue of hippocampal function, chronic fluoxetine treatment also rescued the LTP deficit induced by the T7 cycle (Fig. 3d). Subchronic fluoxetine treatment did not rescue the increased depression or learning defect observed in mice housed in the T7 cycle (Supplementary Fig. 8), consistent with published reports¹⁷. We also used desipramine, a tricyclic antidepressant, and found that desipramine restored learning (Supplementary Fig. 9 and Supplementary Information). These results show that the detrimental behavioural changes induced by aberrant light exposure can be alleviated with antidepressant administration.

To determine the mechanism by which fluoxetine restores learning, we measured the circadian period in T7 mice treated with fluoxetine.

similar basal synaptic release properties ($P_{\text{interaction}} = 0.7256$) ($n = 5$ per group) (fibre volley: $P_{\text{interaction}} = 0.984$, slope: $P > 0.1$). EPSP; excitatory postsynaptic potential; ISI, interstimulus intervals; PPF, paired-pulse facilitation. **g–i**, T7 mice showed LTP deficits ($n = 5$ per group, 1 TBS: $P_{\text{interaction}} < 0.01$; 4 TBS: $P_{\text{interaction}} < 0.01$) (**g** and **h**) but no difference in LTD (**i**). ppLFS, paired-pulse low-frequency stimulation. **j**, T7 mice showed deficit in novel object recognition (T24: $n = 24$, $P = 0.0057$; T7: $n = 24$, $P = 0.1773$). * $P < 0.05$; ** $P < 0.01$. Error bars indicate s.e.m.

Although fluoxetine can phase shift the circadian oscillator¹⁸, chronic administration of fluoxetine did not change the length of the circadian period in mice housed in the T7 cycle (Supplementary Fig. 10). We then examined the corticosterone rhythms in fluoxetine-treated T7 mice and showed that corticosterone rhythms persist with lower overall levels compared with untreated mice (Fig. 3e). These data indicate that fluoxetine treatment does not alter circadian rhythms but instead lowers the level of corticosterone, which could lead to lower depression-like behaviour and better learning.

Studies have suggested that ipRGCs, in addition to affecting reflexive, irradiance-dependent non-image forming visual functions, might directly influence higher cognitive functions and brain processing of emotions^{19–22}. To determine directly whether ipRGCs mediate the effects of the T7 cycle on mood and learning, we tested mice lacking ipRGCs (*Opn4^{aDTA/dDTA}*, herein referred to as aDTA mice). Although most ipRGCs are ablated, these mice still retain more than 95% of RGCs and are capable of image formation⁵. First, we compared wild

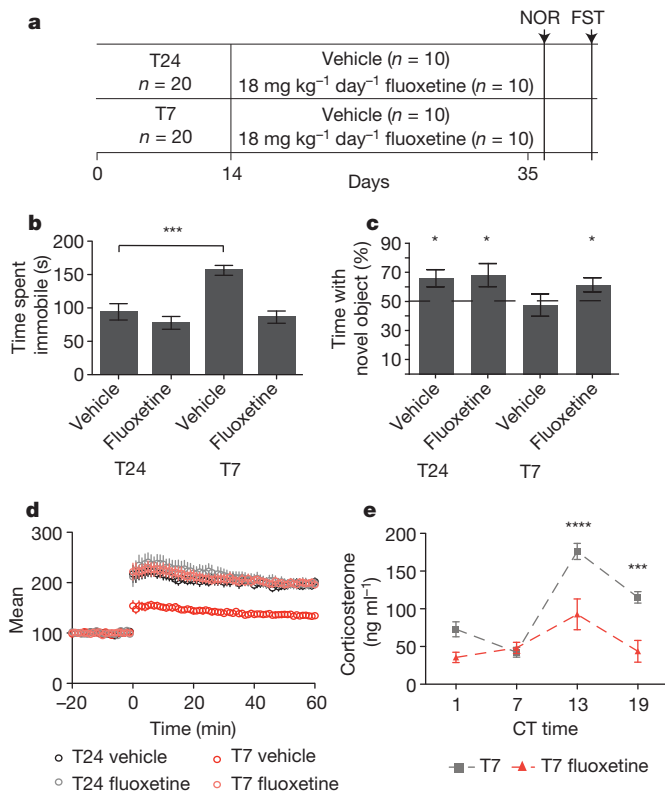


Figure 3 | Chronic antidepressant administration rescues learning.

a, Timeline for fluoxetine administration and testing. NOR, novel object recognition. **b**, Chronic fluoxetine reduced T7 immobility time in the FST ($n = 10$ per group, $P_{\text{interaction}} = 0.0092$, Bonferroni post-test: $P < 0.001$ T24 versus T7 vehicle). **c**, T7 mice treated with fluoxetine showed restored novel object preference (T24_{vehicle}: $n = 9$, $P = 0.03$; T24_{fluoxetine}: $n = 9$, $P = 0.048$; T7_{vehicle}: $n = 10$, $P = 0.77$; T7_{fluoxetine}: $n = 10$, $P = 0.04$). **d**, Chronic fluoxetine rescued the T7-induced LTP deficit ($n = 5$ (T24 vehicle), $n = 5$ (T24 fluoxetine), $n = 5$ (T7 vehicle), and $n = 4$ (T7 fluoxetine); $P_{\text{interaction}} < 0.0001$). **e**, Chronic fluoxetine decreased corticosterone levels in T7 mice ($n = 5$ –8 per time point). T7 corticosterone levels are plotted for comparison. ($P_{\text{interaction}} = 0.0053$, Bonferroni post-test: $P < 0.0001$ CT 13 and $P < 0.001$ CT 19). * $P < 0.05$; *** $P < 0.001$; **** $P < 0.0001$. Error bars indicate s.e.m.

type to aDTA littermates and showed no differences in baseline for the FST and corticosterone levels (Supplementary Fig. 11). We then placed aDTA mice under T24 and T7 cycles and found no difference in anxiety-like behaviours between the two groups (Supplementary Fig. 12). By contrast, the increased depression-like behaviour, learning deficits and hippocampal LTP decrement observed in the T7 cycle in wild-type animals were not observed in aDTA mice exposed to this cycle (Fig. 4). These results indicate that the negative influence of the aberrant light cycles on behaviour requires ipRGCs. Thus, subconscious light detection in humans via ipRGCs may be responsible for the depression and learning deficits observed under disruptive light environments.

Manipulation of the light environment can lead to disruptions in circadian rhythms and sleep and also cause mood and learning defects in mice and humans^{2,23,24}. These studies have led to a model in which light affects cognition exclusively through the modulation of sleep and circadian pathways (Supplementary Fig. 13). Here, we provide a further model in which light directly influences mood leading to learning deficits in the context of an intact circadian timing system and normal sleep distribution and architecture (Supplementary Fig. 13a). Further support that the effects of the T7 cycle are not due to circadian disruptions originate from behavioural comparisons to animals lacking a functional circadian oscillator (for example, circadian mutant- or SCN lesioned- animals), in which reduced depression-like behaviour is observed^{25,26} (Supplementary Fig. 13b). Taken together,

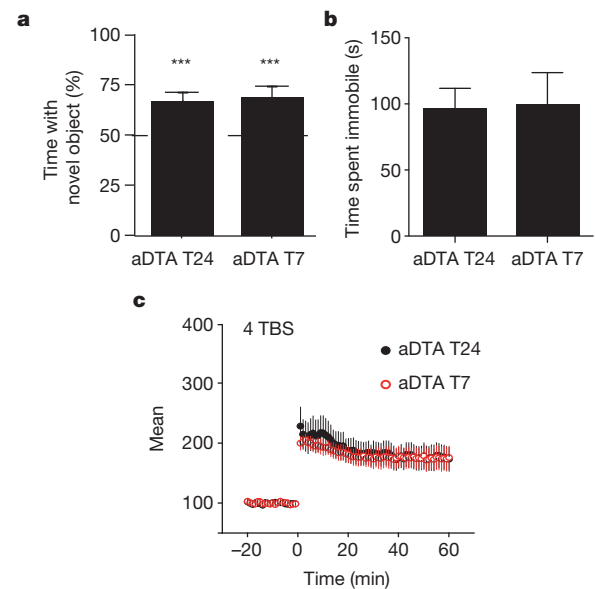


Figure 4 | ipRGCs mediate impairment of mood and learning by aberrant light. **a**, Mice lacking ipRGCs showed a significant preference for the novel object when housed in both the T24 and T7 light cycles ($n = 12$ per group, $P < 0.001$). **b**, aDTA mice housed in the T7 cycle performed similarly to those housed in the T24 cycle in the FST ($n = 6$ (T24) and $n = 5$ (T7), unpaired t -test: $P = 0.93$). **c**, T7 aDTA mice had similar LTP to T24 aDTA mice in response to four-pulse TBS. *** $P < 0.001$. Error bars indicate s.e.m.

these data provide evidence that the aberrant light effects on mood are direct. Furthermore, the depression-like behaviour caused by the T7 aberrant light cycle can serve as an alternative experimental model for depression research in rodents, independent of genetic manipulations or aversive treatments such as repetitive restraint or electric shocks.

METHODS SUMMARY

Adult (4–8 months) male mice (B6/129 F₁ hybrid; Jackson Laboratory) were used for all experiments involving wild-type mice placed under different light environments. Adult littermate aDTA mice placed under different light environments were of B6/129 background (6–8 months) and were raised in our laboratory. aDTA mice could not be used until they were at least 6 months old because elimination of the melanopsin cell population in these mice is not complete until this time⁵. All mice were individually housed in standard animal facility cages with access to food and water *ad libitum*. All mice were initially entrained to a 12 h:12 h light–dark cycle (T24), after which the lights for one group were switched to a 3.5 h:3.5 h light–dark cycle (T7) for 2 weeks. The light intensity during the light portion was ~ 800 lux, chosen to cause no circadian arrhythmicity. All experiments were done in accordance with the regulations set forth by Johns Hopkins University and Rider University Animal care and use committee.

Behavioural analysis. Mice were maintained in the T24 or T7 light cycle for 2 weeks before testing unless otherwise indicated. Body temperature and general activity were measured to evaluate circadian rhythmicity. Sucrose preference and the FST were used to assess depression-like behaviour. The MWM and novel object recognition test were used to assess hippocampal-dependent learning.

Cellular and molecular analysis. To examine the circadian timing system, immunohistochemistry and qRT–PCR were used to quantify PER2 expression in the SCN and liver, respectively. Serum corticosterone levels were quantified by ELISA. Electrophysiological recordings from the dorsal hippocampus were performed to evaluate hippocampal function including LTP and LTD.

Full Methods and any associated references are available in the online version of the paper.

Received 4 April 2011; accepted 11 October 2012.

Published online 14 November 2012.

- Reppert, S. M. & Weaver, D. R. Coordination of circadian timing in mammals. *Nature* **418**, 935–941 (2002).
- Foster, R. G. & Wulff, K. The rhythm of rest and excess. *Nature Rev. Neurosci.* **6**, 407–414 (2005).

3. Berson, D. M., Dunn, F. A. & Takao, M. Phototransduction by retinal ganglion cells that set the circadian clock. *Science* **295**, 1070–1073 (2002).
4. Hattar, S., Liao, H. W., Takao, M., Berson, D. M. & Yau, K. W. Melanopsin-containing retinal ganglion cells: architecture, projections, and intrinsic photosensitivity. *Science* **295**, 1065–1070 (2002).
5. Güler, A. D. *et al.* Melanopsin cells are the principal conduits for rod–cone input to non-image-forming vision. *Nature* **453**, 102–105 (2008).
6. Hattar, S. *et al.* Central projections of melanopsin-expressing retinal ganglion cells in the mouse. *J. Comp. Neurol.* **497**, 326–349 (2006).
7. Altimus, C. M. *et al.* Rods-cones and melanopsin detect light and dark to modulate sleep independent of image formation. *Proc. Natl Acad. Sci. USA* **105**, 19998–20003 (2008).
8. Lam, R. W. & Levitan, R. D. Pathophysiology of seasonal affective disorder: a review. *J. Psychiatry Neurosci.* **25**, 469–480 (2000).
9. Nestler, E. J. *et al.* Neurobiology of depression. *Neuron* **34**, 13–25 (2002).
10. McEwen, B. S. Protective and damaging effects of stress mediators. *N. Engl. J. Med.* **338**, 171–179 (1998).
11. Cryan, J. F. & Holmes, A. The ascent of mouse: advances in modelling human depression and anxiety. *Nature Rev. Drug Discov.* **4**, 775–790 (2005).
12. Baldi, E., Lorenzini, C. A. & Corrado, B. Task solving by procedural strategies in the Morris water maze. *Physiol. Behav.* **78**, 785–793 (2003).
13. Vorhees, C. V. & Williams, M. T. Morris water maze: procedures for assessing spatial and related forms of learning and memory. *Nature Protocols* **1**, 848–858 (2006).
14. Bliss, T. V. & Collingridge, G. L. A synaptic model of memory: long-term potentiation in the hippocampus. *Nature* **361**, 31–39 (1993).
15. McDermott, C. M. *et al.* Sleep deprivation causes behavioral, synaptic, and membrane excitability alterations in hippocampal neurons. *J. Neurosci.* **23**, 9687–9695 (2003).
16. Honey, R. C., Watt, A. & Good, M. Hippocampal lesions disrupt an associative mismatch process. *J. Neurosci.* **18**, 2226–2230 (1998).
17. Dulawa, S. C., Holick, K. A., Gundersen, B. & Hen, R. Effects of chronic fluoxetine in animal models of anxiety and depression. *Neuropsychopharmacology* **29**, 1321–1330 (2004).
18. Sprouse, J., Braselton, J. & Reynolds, L. Fluoxetine modulates the circadian biological clock via phase advances of suprachiasmatic nucleus neuronal firing. *Biol. Psychiatry* **60**, 896–899 (2006).
19. Lockley, S. W. *et al.* Short-wavelength sensitivity for the direct effects of light on alertness, vigilance, and the waking electroencephalogram in humans. *Sleep* **29**, 161–168 (2006).
20. Vandewalle, G. *et al.* Spectral quality of light modulates emotional brain responses in humans. *Proc. Natl Acad. Sci. USA* **107**, 19549–19554 (2010).
21. İyilikci, O., Aydın, E. & Canbeyli, R. Blue but not red light stimulation in the dark has antidepressant effect in behavioral despair. *Behav. Brain Res.* **203**, 65–68 (2009).
22. Warthen, D. M., Wiltgen, B. J. & Provencio, I. Light enhances learned fear. *Proc. Natl Acad. Sci. USA* **108**, 13788–13793 (2011).
23. Fonken, L. K. *et al.* Influence of light at night on murine anxiety- and depressive-like responses. *Behav. Brain Res.* **205**, 349–354 (2009).
24. Ma, W. P. *et al.* Exposure to chronic constant light impairs spatial memory and influences long-term depression in rats. *Neurosci. Res.* **59**, 224–230 (2007).
25. Roybal, K. *et al.* Mania-like behavior induced by disruption of CLOCK. *Proc. Natl Acad. Sci. USA* **104**, 6406–6411 (2007).
26. Tataroğlu, O., Aksoy, A., Yilmaz, A. & Canbeyli, R. Effect of lesioning the suprachiasmatic nuclei on behavioral despair in rats. *Brain Res.* **1001**, 118–124 (2004).

Supplementary Information is available in the online version of the paper.

Acknowledgements We would like to thank T. Gould, G. Ball and A. Sawa for their expert advice on the behavioural tests. We would like to thank R. Kuruvilla for her critical reading and advice on this manuscript. We would also like to thank the mouse tri-laboratory for suggestions and advice. This work was supported by the David and Lucile Packard Foundation grant to S.H.

Author Contributions T.A.L., C.M.A., H.Z., E.T.W. and S.H. designed experiments. T.A.L. and C.M.A. carried out experiments. H.W., H.-K.L., S.Y. and A.K. designed and performed electrophysiological experiments. T.A.L., C.M.A., H.Z., E.T.W. and S.H. wrote the paper.

Author Information Reprints and permissions information is available at www.nature.com/reprints. The authors declare no competing financial interests. Readers are welcome to comment on the online version of the paper. Correspondence and requests for materials should be addressed to S.H. (shattar@jhu.edu).

METHODS

Animals and housing. Adult (4–8 months) male mice (B6/129 F₁ hybrid; Jackson Laboratory) were used for all experiments involving wild-type mice placed under different light environments. Adult littermate aDTA mice placed under different light environment were of B6/129 background (6–8 months) and were raised in our laboratory. aDTA mice could not be used until they were at least 6 months old because elimination of the melanopsin cell population in these mice is not complete until this time⁵. All mice were individually housed in standard animal facility cages with access to food and water *ad libitum*. All mice were initially entrained to a 12 h:12 h light–dark cycle (T24), after which the lights for one group were switched to 3.5 h:3.5 h light–dark (T7) for 2 weeks. The light intensity during the light portion was ~800 lx, chosen to have no circadian arrhythmicity. All experiments were done in accordance with the regulations set forth by Johns Hopkins University and Rider University Animal care and use committee.

Body temperature measurements. Body temperature measurements were made using G2 E-mitter telemetric probes from Mini Mitter (Respironics). The telemetric probe was implanted into the peritoneum and sutured to the inside of the abdominal wall. Mice were given 1 week to recover from surgery before any recording.

Recordings were obtained using Vitalview software (Respironics), at a rate of 30 measurements per hour. Throughout, experiment mice were maintained in their home cage without perturbation and the light cycles were adjusted to test response to both the T24 and T7 light cycles. Circadian period was determined by fitting a regression line to the onsets of activity over a 7-day period using Clocklab (Actimetrics). Period lengths of mice housed in the T24 and T7 light cycles were compared using an unpaired Student's *t*-test.

General activity measurements. General activity was measured using infrared motion detectors from Mini Mitter (Respironics). Mice were housed individually, and the motion detector was mounted to the top of the cage so that general activity could be monitored throughout the T24 and T7 light cycle. Data were collected in 10-min bins using Vitalview software (Respironics). Circadian period length was determined by fitting a regression line to the onsets of activity over a 7-day period using Clocklab (Actimetrics). Period lengths of mice housed in the T24 and T7 light cycles were compared using an unpaired Student's *t*-test.

Molecular rhythm measurements. Mice were housed in either the T24 ($n = 16$) or the T7 ($n = 16$) light cycle for 2 weeks, during which general activity was monitored in T7 mice to determine their circadian phase. Mice were sampled across four time points. Mice under the T24 cycle were sampled at ZT 1, 7, 13 and 19, and mice under the T7 cycle were sampled at CT 1, 7, 13 and 19, which was determined using their general activity rhythm. Each mouse was removed from its cage, and tail blood was quickly sampled. The mouse was then anaesthetized with 1 ml of avertin (20 mg ml⁻¹). Once anaesthetized, a small sample of liver was isolated. The mouse was then perfused transcardially with 0.9% saline followed by 4% paraformaldehyde. The brain was removed and postfixed overnight in 4% paraformaldehyde followed by cryoprotection and embedding in OCT compound (Sakura Finetek).

Real-time PCR. Liver samples were homogenized and RNA extracted using the RNeasy mini kit (Qiagen). The Retroscript kit (Ambion) was used to reverse transcribe poly(A) RNAs. Real-time quantitative PCR was performed with iQ SYBR Green Supermix and the iCycler iQ real-time PCR detection system (Bio-Rad). Each sample was analysed in triplicate reactions of 50 µl. Primers for *Per2* were forward: 5'-GCCTTCAGACTCATGATGACAGA-3' and reverse: 5'-TTTGTGTGCGTCAGCTTTGG-3'. Primers for 18S rRNA (internal control) were forward: 5'-CGCCGCTAGAGGTGAAATTC-3' and reverse: 5'-TTGGCAAATGCTTTTCGCTC-3'.

Data were analysed using the $\Delta\Delta C_t$ method, normalizing each sample to the internal control, and relative messenger RNA was determined as the percentage of the maximum value observed in the experiment. Data were analysed by two-way analysis of variance (ANOVA) followed by a Bonferroni post-hoc test to examine differences over time as well as potential light cycle effects on *Per2* expression.

PER2 immunohistochemistry. Brains were sectioned (40 µm) by cryostat through the rostral–caudal extent of the SCN, and were stored free floating in 0.1 M phosphate buffer. Free-floating sections were incubate in blocking buffer (0.1 M phosphate buffer, 3% triton, 0.5% bovine serum albumin and 1% goat serum) for 2 h. Sections were then incubated in rabbit anti-Per2 (Alpha Diagnostic International; 1:4,000 in blocking buffer) overnight and visualized with a Vectastain horseradish peroxidase kit (Vector Labs) using 3,3'-diaminobenzidine (DAB; Sigma). Sections were mounted on microscope slides, dehydrated and coverslipped with Permount. Sections were imaged at $\times 10$ magnification with a Zeiss Axio Imager M1 microscope. Optical density was measured using ImageJ. Data were analysed by two-way ANOVA followed by a Bonferroni post-hoc test to examine differences over time as well as potential light cycle effects on PER2 expression.

Corticosterone measurement. Serum was isolated from collected tail blood and assayed for corticosterone by ELISA (Assaypro). Data were analysed by two-way ANOVA followed by a Bonferroni post-hoc test to examine differences over time as well as light cycle effects on corticosterone levels. For fluoxetine experiments, corticosterone levels were analysed by two-way ANOVA followed by a Bonferroni post-hoc to examine differences over time as well as the effect of fluoxetine.

For the experiment comparing wild-type and aDTA mice, serum was sampled from wild-type and aDTA mice at ZT 13/CT 13 based on general activity rhythms (as described above). The samples were processed as described above. Corticosterone levels of wild-type and aDTA mice were analysed by unpaired Student's *t*-test.

Light-induced c-Fos expression. Mice were housed under a 12 h:12 h light–dark cycle and were exposed to a 10-min light pulse at ZT 14 (2 h after light offset), after which they were placed back in the dark for a further 80 min. Control mice remained in the dark until anaesthetization. Ninety minutes after the start of light presentation, mice were deeply anaesthetized with 1 ml of avertin (20 mg ml⁻¹). Once anaesthetized, the mice were perfused transcardially with 0.9% saline followed by 4% paraformaldehyde. Brains were removed, postfixed overnight in 4% paraformaldehyde, and then transferred to 0.1 M phosphate buffer. Brains were sectioned (40 µm) through the rostro–caudal extent of the SCN using a vibratome (World Precision Instruments). Sections were stored free floating in 0.1 M phosphate buffer. Every other section was stained immunohistochemically for c-Fos. Sections were incubated in blocking buffer (0.1 M phosphate buffer, 3% Triton X-100 and 0.5% bovine serum albumin) for 2 h. Sections were incubated in rabbit anti-c-Fos (Calbiochem Ab-5; 1:20,000) overnight at 4 °C and then visualized with a goat anti-rabbit Vectastain horseradish peroxidase kit (Vector Labs) using DAB (Sigma) as a chromagen. Sections were mounted on microscope slides, dehydrated and coverslipped with Permount. Slides were viewed and imaged on a Zeiss Axio Imager.M1 microscope at $\times 5$ magnification. Photoshop and ImageJ were used to count c-Fos-positive cells and measure the area of region counted from. The number of c-Fos positive cells was normalized to the area of the region, and these values were compared between mice that received a light pulse and dark controls. These data were analysed using an unpaired Student's *t*-test.

Sucrose anhedonia. Mice were housed in the presence of two water bottles 1 day before testing to acclimate them to the bottles. Sucrose preference was assessed over 2 days. Each day, one bottle containing 1% sucrose and one bottle containing water were introduced at the beginning of the active phase. The position of these bottles was switched 6 h later, and the bottles were removed at the end of the active phase. Bottles were weighed at the beginning and end of the active period to measure amount consumed. Sucrose preference was calculated by dividing the amount of sucrose consumed by the total amount consumed (water and sucrose). The percentage of sucrose consumed by mice in the T24 and T7 cycles was compared by a Student's *t*-test.

FST. Mice were individually placed in an inescapable container of water (25 °C) for 6 min. Behaviour was monitored by video cameras positioned in front of the apparatus and scored by a video tracking system (Forced Swim Test, Bioserve). Time spent immobile for the last 4 min of the test was calculated. Increased time spent immobile is indicative of increased depression-related behaviour. The amount of time spent immobile during the last 4 min was analysed by Student's *t*-test. For fluoxetine experiments, the amount of time spent immobile during the last 4 min were analysed by two-way ANOVA followed by a Bonferroni post-hoc to compare light cycle and drug treatment.

Open field. Mice were individually placed in the centre of a large, brightly lit arena (500 lx, 60 \times 60 cm) and allowed to explore for 5 min. Behaviour was monitored from above by a video camera connected to a computerized video tracking system (Anymaze, Stoelting). The apparatus was cleaned thoroughly between each trial. The percentage distance travelled and time in the centre of the arena were measured. These measures were compared between mice housed in the T24 and T7 cycles using an unpaired Student's *t*-test.

Light–dark box. The light–dark box consisted of two compartments equivalent in size (20 \times 20 cm); one area is brightly lit (600 lx) and the other is dimly lit (<1 lx). A small opening joins the two compartments, so the mice could freely move between the two areas. Mice were dark adapted for 1 h before testing. At the beginning of the test, dark-adapted mice were placed in the lit compartment facing away from the opening and allowed to freely explore for 5 min. Behaviour was monitored from above by a video camera connected to a computerized video tracking system (Anymaze). The apparatus was cleaned thoroughly between each trial. The number of transitions between the two compartments as well as the time spent and distance travelled in the lit room were measured as indications of anxiety-related behaviour. These measures were compared between mice housed in the T24 and T7 cycles using an unpaired Student's *t*-test.

Elevated plus maze. The apparatus consisted of two open arms (42 \times 6 cm) opposite to one another and two arms enclosed by walls (42 \times 6 \times 14 cm) opposite

of one another forming a cross. The arms were separated by a central platform (6×6 cm). The maze was elevated (33 cm) such that the open arms convey openness, unfamiliarity and elevation. The light intensity in the open arms was ~ 600 lx, whereas the light intensity in the closed arms was ~ 200 lx. Mice were placed in the centre of the elevated plus maze facing one of the open arms. Behaviour was monitored from above by a video camera connected to a computerized video tracking system (Anymaze). The apparatus was cleaned thoroughly between each trial. The time spent and the distance travelled in the open arms were measured as indications of anxiety-related behaviour. These measures were compared between mice housed in the T24 and T7 cycles using an unpaired Student's *t*-test.

MWM. The water maze consisted of a circular pool (150 cm in diameter) with room temperature water ($26\text{--}28^\circ\text{C}$). The water was made opaque with the addition of non-toxic white tempura paint to hide the escape platform. The platform was made from PVC piping with a top (10 cm in diameter) painted white and submerged in the pool such that 1 cm of water covered the platform hiding it from sight. For visual trials, a flag made from a 50-ml conical tube covered with coloured tape was placed on the platform. During the acquisition, probe and reversal trials, four cues were attached to the side of the pool equidistant from one another, and the entire pool was surrounded by a plain curtain to block any other visual cues. Performance was scored using a video tracking system (Anymaze) with a camera mounted above the pool. The light intensity at the water surface was approximately 500 lx.

Mice were tested in four stages: visual, acquisition, probe and reversal (see Fig. 2a). Before spatial training, mice were trained to escape the pool using the visual flag located on top of the platform to familiarize them with the test. This was performed four times with an inter-trial interval of (30 min), and the platform was moved between each trial. We also used this visual training to screen for and remove animals that show floating behaviour in the water maze. Animals that floated in two or more trials during training were not tested in the spatial task to prevent confounds from floating behaviour. During the acquisition phase, mice were trained (one trial per day for 12 days) to find the hidden platform using the four visual distal cues surrounding the pool. The mouse was randomly placed in a different area of the pool at the start of each trial with the platform maintained in the same quadrant (target quadrant). The platform was removed on day 13 in the probe trial. The swimming in each quadrant and specifically the preference for the target quadrant was measured to evaluate spatial memory using a computerized video tracking system (Anymaze). Reversal training began on day 14 when the platform was moved to the quadrant opposite the original target quadrant. Mice were trained as described for the acquisition phase.

Latency to locate the platform during the acquisition and reversal phases was analysed by two-way ANOVA followed by a Bonferroni post-hoc test to examine changes in latency throughout the course of the experiment as well as the effect of light cycle exposure. Probe trial was analysed by calculating the percentage time spent in the target quadrant and performing a one-sample *t*-test to determine whether this was significantly above 25%.

Novel object recognition. Novel object recognition was composed of three stages: acclimation to the novel object arena, familiar object exposure and finally novel object exposure. Mice were first removed from their home cage, acclimated to the empty testing arena (light intensity of 500 lx) for 10 min, and subsequently returned to their home cage 24 h before including two objects in the arena. The day after acclimation, mice were returned to this arena with two identical objects that they could freely explore for 10 min, after which they were returned to their home cage for 1 h. At the end of the 1-h period, mice were placed back into the arena with one of the objects changed to a novel object, and were allowed to

explore both the familiar and novel objects for 5 min. Behaviour was monitored from above by a video camera connected to a computerized video tracking system (Anymaze), and the percentage of time spent with each object was calculated. Wild-type mice spend more time with the novel object, however, mice with recognition memory deficits will not be able to distinguish the novel from the stable object. Objects had been previously tested to ensure that animals showed no initial preference for a particular object. The identity of the objects (familiar versus novel) was counterbalanced. The objects and arena were thoroughly cleaned between each trial to remove odour cues. Object recognition was analysed by calculating the percentage time spent with the novel object and performing a one sample *t*-test to determine whether this was significantly above 50%.

Slice electrophysiology. Coronal (0.4 mm) hippocampal slices were prepared as described²⁷ in ice-cold dissection buffer (2.6 mM KCl, 1.23 mM NaH_2PO_4 , 26 mM NaHCO_3 , 212.7 mM sucrose, 10 mM dextrose, 3 mM MgCl_2 and 1 mM CaCl_2 , bubbled with 5% CO_2 , 95% O_2). Recordings were done in a similar buffer but with the sucrose replaced by NaCl and the temperature raised to 30°C . Synaptic responses were evoked at 0.33 Hz stimulating the Schaffer collaterals with 0.2-ms pulses (concentric bipolar electrodes, FHC), and recorded extracellularly in CA1 stratum radiatum. LTP was induced by TBS, consisting of one or four theta epochs delivered at 0.1 Hz. Each epoch, in turn, consisted of 10 trains of four pulses (at 100 Hz) delivered at 5 Hz. LTD was induced by low frequency stimulation (1 Hz, 15 min). These protocols were delivered after 20 min of stable baseline transmission. All hippocampal slice electrophysiological recordings were performed and analysed by an experimenter blind to the treatment of the animals. Two-way ANOVA was used to analyse fibre volley differences between the T7 and T24 treatments. The slopes for the linear fit of the fibre-volley-slope relationship were compared by *t*-test.

Fluoxetine administration. Mice were housed in either the T24 or T7 cycle for two weeks ($n = 20$ per group) with food and water *ad libitum*. For chronic treatment, this was followed by a 3-week treatment of $18\text{ mg kg}^{-1}\text{ day}^{-1}$ of fluoxetine (Sigma). For subchronic treatment, this was followed by a 4-day treatment of $18\text{ mg kg}^{-1}\text{ day}^{-1}$. Fluoxetine was administered in the drinking water and control mice received tap water. Dosage was calculated based on the average amount of water consumed per day and mouse weight. Fluoxetine consumption was also measured during treatment to determine the amount consumed per mouse.

Period length measurement with fluoxetine treatment. Mice were housed under infrared motion detectors as described above. Mice were housed in the T7 light cycle for 2 weeks after which fluoxetine ($18\text{ mg kg}^{-1}\text{ day}^{-1}$) was administered in the drinking water for 3 weeks. Circadian period was determined by fitting a regression line to the onsets of activity over a 7-day period. Period lengths before and after 3 weeks of fluoxetine treatment were compared by paired *t*-test.

Desipramine administration. Desipramine (Sigma) was dissolved in sterile water with 5% Tween-20. Each mouse received 16 mg kg^{-1} desipramine intraperitoneally 24- and 1-h before testing in the novel object recognition paradigm. The same volume of vehicle (water with 5% Tween-20) was administered intraperitoneally to control mice.

Statistical analysis. All statistical analysis was performed using GraphPad Prism. Specific tests used to analyse data are described their respective section of the methods.

- Lee, H. K., Min, S. S., Gallagher, M. & Kirkwood, A. NMDA receptor-independent long-term depression correlates with successful aging in rats. *Nature Neurosci.* **8**, 1657–1659 (2005).